

## Atomic interdiffusion at Au-GaAs interfaces studied with Al interlayers

L. J. Brillson

*Xerox Webster Research Center, 800 Phillips Road W114, Webster, New York 14580*

Robert S. Bauer, R. Z. Bachrach, and G. Hansson

*Xerox Palo Alto Research Center, 3333 Coyote Hill Road, Palo Alto, California 94304*

(Received 27 June 1980; revised manuscript received 12 December 1980)

We have used soft-x-ray photoemission spectroscopy at Au/GaAs interfaces to determine the movement of Au, Ga, and As atoms during the initial stages of Schottky-barrier formation. Studies of core-level features obtained with a range of photon energies between 80 and 250 eV indicate that, at room temperature, Au atoms first diffuse into GaAs, followed by the nonstoichiometric outdiffusion of Ga and As into Au overlayers. Thin Au overlayers on GaAs promote a spatial distribution of dissociated Ga and As which depends on the overlayer thickness. These microscopic phenomena result in a local charge redistribution which determines the electronic properties of the macroscopic Au/GaAs junction. We discuss the application of Al atoms at the intimate metal-semiconductor interface either as immobile markers to establish the absolute motion of interface species on an atomic scale or as indicators of the overall interface motion.

### I. INTRODUCTION

The movement of metal and semiconductor atoms near their interface is of growing significance in the understanding of Schottky-barrier formation. A variety of experiments with ultrahigh-vacuum (UHV)-cleaved surfaces of Si,<sup>1,2</sup> III-V,<sup>3-11</sup> and II-VI (Refs. 11-14) compound semiconductors all show that the Fermi level within the surface space-charge region moves to its ultimate Schottky-barrier position within the first few Å or less of metal overlayer coverage. It is also known that extensive interdiffusion can take place between metal and semiconductor, even at room temperature.<sup>15,16</sup> Such interdiffusion is particularly pronounced for relatively unreactive systems such as Au on GaAs,<sup>7,8,17-31</sup> where no reacted interface layer forms<sup>14,32,33</sup> to retard atomic transport.<sup>34</sup> In turn, the atomic redistribution can result in electrically active sites within the semiconductor, which play a role in Schottky-barrier formation. These phenomena emphasize the importance of determining changes in atomic position and bonding near metal-semiconductor interfaces.

In this paper, we present results of soft x-ray photoemission spectroscopy (SXPS) studies of Au-GaAs interdiffusion during the initial stages of Schottky-barrier formation. In particular, we identify the movements of Au, Ga, and As atoms near the Au-GaAs interface with the dramatic electronic changes<sup>5,8,11,29,30</sup> induced by the first few monolayers of Au on UHV-cleaved GaAs surfaces. We have employed a novel approach to characterize absolute atomic movement. This method employs SXPS to monitor metal and semiconductor atom movement relative to interlayer Al atoms adsorbed on the free-surface layer of the

semiconductor prior to depositing the Au metal contact.<sup>35</sup> The interlayer Al atoms permit diffusion of semiconductor atoms into the metal to be distinguished from diffusion of metal atoms into the semiconductor if their position is fixed. Even if large rearrangement of the initial Al-GaAs interface were to occur, the relative movements of semiconductor atoms relative to the Au contact can be discerned. Such determination is achievable even for displacements of only one or two lattice spacings. The SXPS-marker technique has a precision which is several orders of magnitude greater than those of bulk metallurgical techniques, thereby permitting analysis of diffusion phenomena even at room temperature. An additional feature of this technique is that the chemical-bonding environment of all interface constituents can be monitored by SXPS.

Formation of islands by the metal contact layer does not complicate this analysis. The exposed semiconductor atoms between metal islands are normalized by the corresponding surface concentration of interlayer atoms also exposed. Only the change of SXPS intensities of semiconductor atoms relative to interlayer atoms within any island contributes to the measurement. Even this complication is absent for Au-GaAs interfaces, where Au appears to deposit uniformly with initial deposition.<sup>8,30</sup>

There are several unique advantages to studying interdiffusion with synchrotron radiation. First, the tunable light source permits one to select photon energies such that the kinetic energies of the photoemitted electrons correspond to a minimum in the electron scattering length.<sup>36</sup> Thus, only electrons photoemitted from the top few layer(s) of the surface can successfully escape the solid, re-

sulting in extreme surface sensitivity. By varying the incident photon energy and thereby the escape depth of photoemitted electrons, one can probe the elemental composition on vs just below the metallized semiconductor surface in a nondestructive way.<sup>37</sup> Finally, the chemical shifts of core-level features indicate changes in local chemical bonding during various stages of interdiffusion.

Other techniques of characterizing metal-semiconductor interfaces have serious drawbacks. For example, the depth resolution of Rutherford backscattering spectrometry is typically 150–300 Å for most solids,<sup>38</sup> with atomic information only recently having been obtained. Depth profiling with ion bombardment and Auger electron spectroscopy can achieve higher spatial resolution, e.g., 10–20 Å under optimum conditions.<sup>39</sup> However, sputter sectioning can produce mixing of species,<sup>40</sup> preferential sputtering,<sup>41</sup> and possible triggering of phase transitions<sup>42</sup> caused by intermixing or enhanced reaction rates at interfaces. Electron spectroscopy studies are also undesirable for studying atomic interdiffusion because the incident beam can promote electromigration.<sup>43</sup>

Several previous studies have used markers to study metal-semiconductor interdiffusion. These include discontinuous W films evaporated on Si,<sup>44</sup> inert gas bubbles produced by ion implantation,<sup>45–48</sup> Si isotopes,<sup>49,50</sup> and metal bilayer films.<sup>51</sup> However, these yielded results just on a macroscopic scale. The application of SXPS is the only available method for resolving interdiffusion on a scale of interatomic spacings.

We have used the highly localized bonding observed for Al on UHV-cleaved GaAs in order to mark the Au-GaAs interface. An exchange reaction is believed to occur for Al on GaAs(110) in which Al replaces Ga in the top semiconductor layer.<sup>10,52,53</sup> While the detailed Al bonding to the GaAs surface is not central to the marker technique, a tight-binding calculation based on this exchange geometry yields valence-band, core-level, and interface-dipole features in agreement with experiment.<sup>54,55</sup> Because of the strong AlAs bonding as reflected in the bulk heat of formation ( $-27$  kcal mole<sup>-1</sup>) relative to GaAs bonding ( $-17$  kcal mole<sup>-1</sup>),<sup>56</sup> a relatively inert metal such as Au on this surface can be expected to disrupt primarily GaAs rather than AlAs bonds. Furthermore, the low heat of formation within the Au-Al system ( $-7$  kcal mole<sup>-1</sup>) (Ref. 57) suggests that any Au-Al bonding at the interface is relatively weak. Au-Al phase formation<sup>58</sup> is also unlikely since less than one monolayer of Al atoms (already bonded to the substrate) is available. However, variations in local bonding occur for thin-film reactions,<sup>58</sup> and care must be taken in all chemical analyses.

The Au-GaAs interface is of particular current interest since large interdiffusion effects have been reported for this interface but with conflicting determinations of the primary diffusing species. Using Rutherford backscattering spectrometry of Au on epitaxially grown GaAs, Sinha and Poate found that Ga diffuses to the free surface of Au and that Au diffuses into GaAs upon annealing.<sup>19</sup> Hiraki *et al.* used Auger electron spectroscopy (AES) to determine preferential Ga diffusion to the Au surface from GaAs cleaned in vacuum by Ar<sup>+</sup> bombardment or flash heating. Similarly, Robinson's AES measurements coupled with sputter profiling on (100) epitaxial GaAs indicate preferential Ga outdiffusion and Au indiffusion.<sup>26</sup> Magee and Peng used transmission electron microscopy (TEM) to determine the presence of AuGa crystallization for Au on (100) GaAs single crystals which were polished, etched, and annealed at high temperature.<sup>23</sup> In contrast, x-ray photoemission spectroscopy (XPS) measurements of Waldrop and Grant showed only As present on Au films deposited over Ar<sup>+</sup>-bombarded and annealed (100) GaAs.<sup>59</sup> In addition, SXPS studies of Au on UHV-cleaved (110) GaAs by Chye *et al.*<sup>30</sup> and Lindau *et al.*<sup>8</sup> suggest the outdiffusion of both Ga and As to the free-metal surface in nearly stoichiometric proportions. The lack of consistency between these measurements suggests that chemical preparation of the various Au-GaAs interfaces strongly affects the results and that the bonding at the microscopic interface plays a central role in the process of interdiffusion. Clearly, the above results provide no unambiguous description of atomic movements during the initial stages of Schottky-barrier formation.

The use of interlayer atoms as markers to analyze absolute atomic motion is valid only if the interlayer atoms (a) do not move away from interface during the diffusion process and (b) do not significantly perturb the diffusion process itself. In this paper, we present the nondestructive SXPS depth profile and thickness dependence for submonolayers of Al deposited at Au/GaAs. Interpretations of these data are given which suggest that Au-Al-GaAs satisfy these criteria. However, considerable information concerning the interdiffusion process can be extracted from the SXPS results presented here, regardless of the Al interlayer atom stability. In addition, many of the vital conclusions concerning the absolute movement of the major constituents will be shown to be valid even if the interlayer atoms move below the surface.

In the next section, we describe the experimental apparatus used to carry out SXPS measurements on Au-GaAs interfaces. Section III contains experimental results which describe atomic move-

ments during initial metal deposition on GaAs as well as subsequent spatial distributions. Section IV provides a discussion of these results and their relation to the electronic properties of intimate Au-GaAs interfaces. We highlight those results which depend sensitively on the marker analysis.

## II. EXPERIMENTAL

The SXPS-marker experiments were carried out on the 4° beam line of the Stanford Synchrotron Radiation Laboratory (SSRL). The energy of synchrotron radiation incident at the specimen surface was selected using a double-focus "grass-hopper" monochromator.<sup>60</sup> A UHV chamber (base pressure  $10^{-10}$  Torr) was used in which semiconductor crystals could be cleaved to expose visually smooth surfaces. Single-crystal GaAs doped with  $n = 3.2 \times 10^{17}$  Te cm<sup>-3</sup> from Laser Diode, Inc. were used in this experiment. Thicknesses of Au and Al controllable to fractions of a monolayer were evaporated from W wire sources on to the cleaved GaAs(110) surfaces by rotating the crystal into or out of the evaporant beam. A Sloan quartz-crystal oscillator positioned next to the cleaved surface monitored the thickness of deposited metal. Multiple evaporators were separated by baffles and mounted side by side, so that multilayer metal films could be deposited sequentially in UHV. During metal evaporation, the pressure rose to  $\sim 10^{-9}$  Torr or less. The ionization gauge was kept off during the course of each SXPS experiment to minimize any oxidation of GaAs (Ref. 61) and any photoinduced band-bending effects.<sup>62</sup>

Interdiffusion at Au-Al/GaAs(110) interfaces were studied by monitoring the integrated intensities of the Ga 3*d*, As 3*d*, Al 2*p*, and Au 4*f* core levels as a function of Au and Al evaporated thickness. For a given thickness of Au and Al on GaAs, these core-level intensities were also monitored as a function of photon energy from 80 to 250 eV.

## III. RESULTS

Figure 1 illustrates Ga 3*d*, As 3*d*, and Al 2*p* core-level spectra at  $h\nu = 130$  eV for various metal overlayer thicknesses. For an Al thickness of 1 Å on GaAs(110) [ $0.67 \text{ Å} = \frac{1}{2}$  GaAs(110) surface monolayer], the Al 2*p* core level peaks at 51.4 eV (32 eV to higher binding energy relative to the As 3*d* core-level peak) and exhibits asymmetric broadening toward higher binding energy. The Ga 3*d* core level exhibits a slight broadening and shift to lower binding energy. The As 3*d* core level displayed no measurable shift. The features agree with previous measurements of Al on GaAs(110) in which an exchange reaction is known to occur.<sup>10, 52, 53</sup>

For Al coverages on GaAs of more than a few Å,

the peak position of the Al 2*p* core level shifts to 0.7 eV lower binding energy, corresponding to metallic Al.<sup>10, 52, 53</sup> The absence of this unreacted feature of 1 Å coverage in Fig. 1 indicates that all Al atoms are reacted with the GaAs substrate and that no island formation takes place. Such uniform reacted overlayers also occur for Al on CdS(1010), where only one chemically-shifted core-level feature appears with initial monolayer coverage as well.<sup>63</sup>

With additional deposition of Au over the Al/GaAs surface, the Al 2*p* peak exhibits no change in shape and only a 0.4-eV shift to higher binding energy. This shift is expected since additional charge is transferred from the already bonded Al to the new Au overlayer. No further shift occurs with increasing Au thickness. If Al-As bonds were weakened by the presence of the Au overlayer, one would expect an Al 2*p* peak shifted to lower binding energy, as can be observed for several monolayers of Al on GaAs(110).<sup>10, 52, 53</sup> Likewise, any additional bonding of isolated Al atoms to Au would also result in an Al 2*p* peak shift to lower binding energy due to the weaker Al-Au bonding relative to AlAs. Indeed, a shifted peak was observed in separate studies of Au on GaAs covered with thicker layers of Al.<sup>64</sup> Thus Fig. 1 demonstrates that Au overlayers do not produce any simple dissociation of Al-As bonds at the Al/GaAs interface. We discuss additional evidence in support of this conclusion in Sec. IV.

Figure 1 also shows that Au overlayers on Al/GaAs cause dissociation and diffusion of Ga and As atoms below the GaAs surface. Between 1 Å Al and 8 Å Au + 1 Å Al in Fig. 1, the primary Ga 3*d* peak shifts 1 eV to lower binding energy, indicating the formation of free Ga. Correspondingly, the As 3*d* peak exhibits a 0.7 eV splitting with increasing Au thickness. The smaller peak component shifts to higher binding energy, corresponding to free As, and its intensity increases with increasing Au thickness. This suggests that free As moves toward the Au-vacuum interface and away from the GaAs substrate. Note that the Al interlayer atoms need not remain stationary for these conclusions to be valid. Detailed evidence for such free Ga and As migration will be presented later in this text.

The spectra of the Au 5*d* and 4*f* core levels exhibit features characteristic of "atomiclike" Au dispersed in the GaAs surface, just as found in the case of Au on GaAs(110) with no Al interlayer.<sup>30</sup> Figure 2 illustrates valence-band spectra of cleaved GaAs(110) with successive depositions of Au and Al overlayers and  $h\nu = 130$  eV. With 1 Å Al deposited, the valence-band spectrum exhibits additional structure at 6 eV below the valence-band

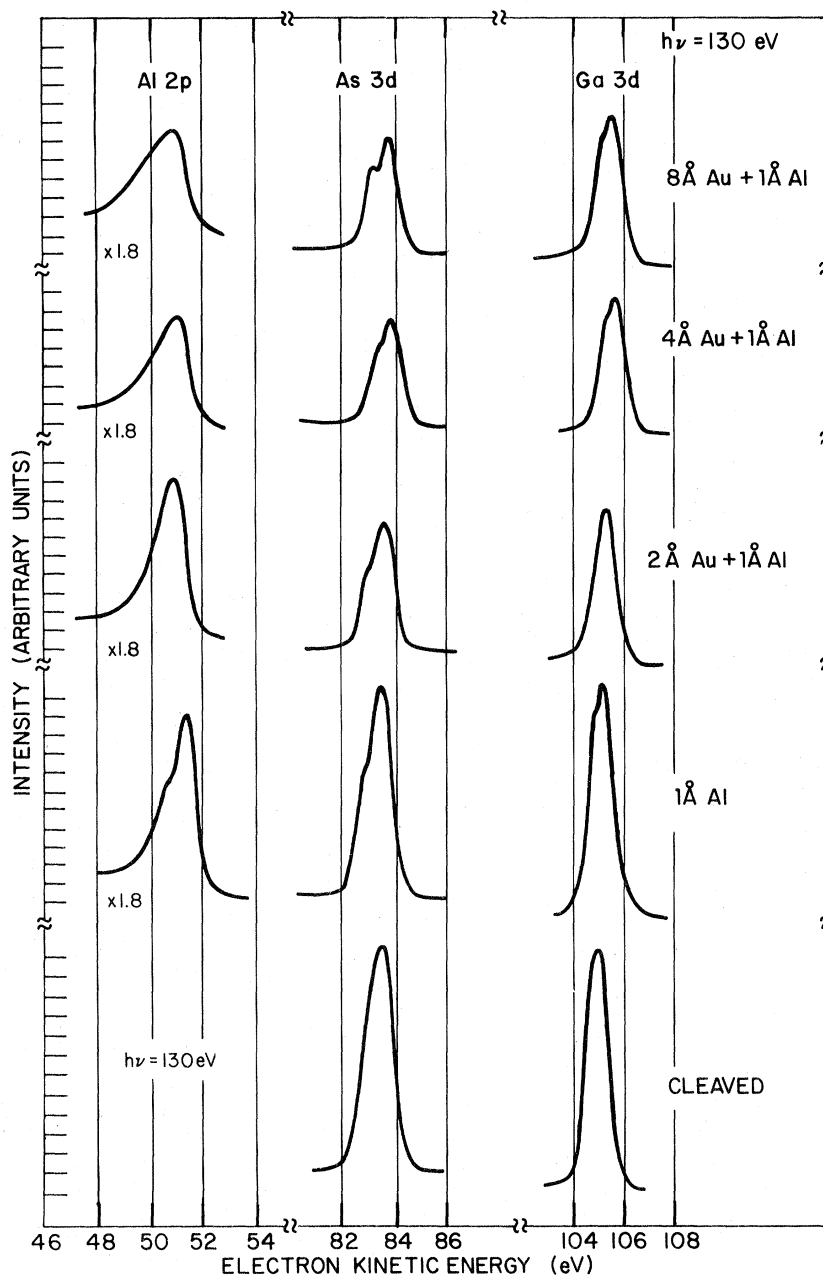


FIG. 1. Photoemission spectra of Al  $2p$ , As  $3d$ , and Ga  $3d$  core levels at  $h\nu = 130$  eV for various Al and Au overlayer coverages.

edge, corresponding to metal-induced interface states and in agreement with previous work.<sup>53</sup> Between the cleaved and 1 Å Al spectra, the extrapolated valence-band edge shifts 0.4–0.5 eV to higher energy, corresponding to an 0.4–0.5 eV increase in surface work function. The same increase in surface work function is measured by contact potential difference and photoemission methods elsewhere.<sup>10,65</sup> Deposition of 2 Å Au pro-

duces two new peak features at 117.6 and 119.3 eV, which correspond to Au  $5d$  levels. Their splitting is 1.7 eV, indicative of Au dispersed within the substrate.<sup>30,66</sup> The Au  $5d$  splitting increases with additional Au deposition, reaching 2.1 eV at 8 Å Au. However, even with several monolayers of Au deposited on Al/GaAs, the Au  $5d$  splitting is still less than the metallic Au splitting of 2.3 eV. This phenomenon is possible only if there is

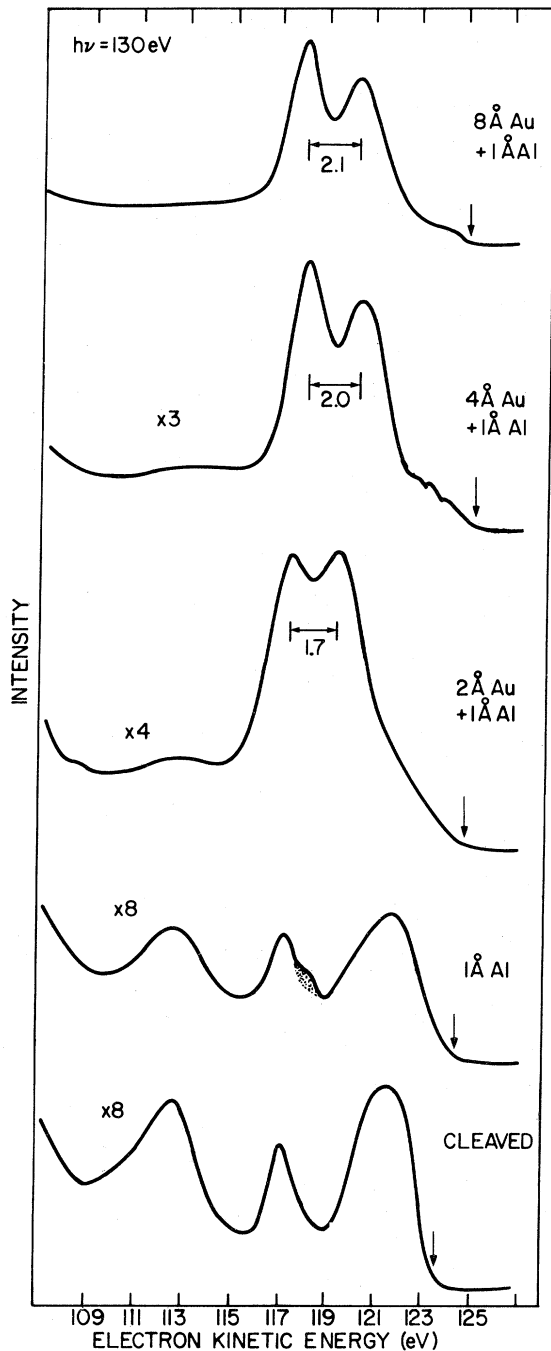


FIG. 2. Photoemission spectra of cleaved GaAs(110) valence band at  $h\nu = 130$  eV for various Al and Au overlayer coverages. Shaded area in  $1 \text{ \AA}$  Al spectrum corresponds to a metal-induced surface state. Arrows denote the valence-band edge in each spectrum.

strong intermingling of Au, Ga, and As over many atomic layers. The presence of Al atoms, no matter where they may be located, will not impact this interpretation.

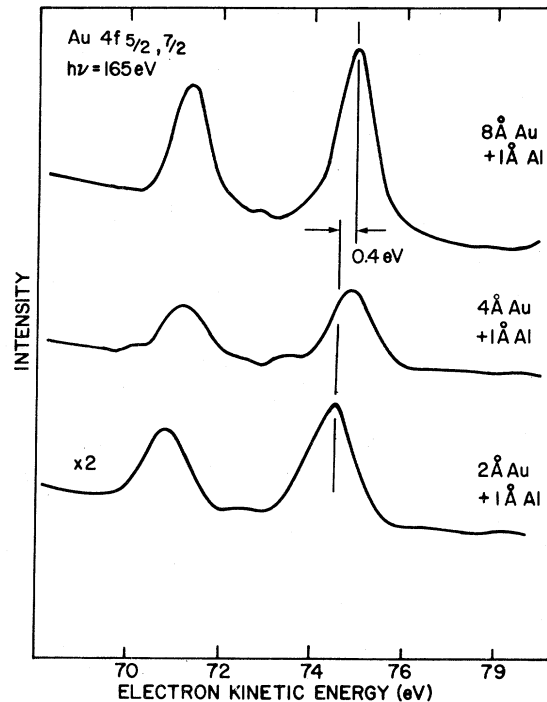


FIG. 3. Photoemission spectra of Au  $4f$  core levels at  $h\nu = 165$  eV for various Au coverages on cleaved GaAs(110) +  $1 \text{ \AA}$  Al.

The Au  $4f$  core levels also show a characteristic shift in binding energy between the dispersed and metallic regimes. This is illustrated in Fig. 3 for surface-sensitive spectra obtained with  $h\nu = 165$  eV. The Au  $4f$  core levels shift  $0.4$  eV to higher kinetic energy as the surface becomes metallic, again in agreement with results of Chye *et al.* for dispersed Au in GaAs.<sup>30</sup> However, the Ga and As  $3d$  core levels also shift rigidly to higher kinetic energy by  $\sim 0.4$  eV with the first  $8 \text{ \AA}$  Au deposition. Since chemical shifts induced by the increasingly metallic Au matrix at or within the GaAs surface should be opposite for Ga and As, the rigid shift of both suggests that band-bending and interface-dipole effects<sup>67</sup> continue to change at Au coverages well above one monolayer.<sup>11</sup> This conclusion is supported by the position of the valence-band edge in Fig. 2, which continues to shift to higher kinetic energy at least up to the first  $4 \text{ \AA}$  of Au deposition.

The presence of the anomalously low Au  $5d$  level splittings for Au coverages up to  $8 \text{ \AA}$  demonstrates that the deposited Au does not form islands. Such islands would exhibit metallic features at the lowest Au coverages.<sup>30</sup> Furthermore, no island formation is expected above this coverage since the integrated Au  $4f$  peak intensity continues to increase exponentially and the core levels exhibit no

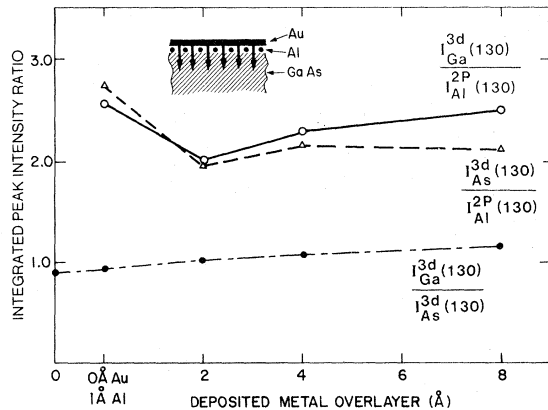


FIG. 4. Integrated peak-intensity ratios  $I_{\text{Ga}}^{3d}(130)/I_{\text{Al}}^{2p}(130)$ ,  $I_{\text{As}}^{3d}(130)/I_{\text{Al}}^{2p}(130)$ , and  $I_{\text{Ga}}^{3d}(130)/I_{\text{As}}^{3d}(130)$  as a function of metal overlayer coverage. The inset illustrates the initial interdiffusion process schematically, assuming immobile Al at the interface. The initial decreases at 2 Å Au coverage correspond to more Au interdiffusion than Ga and As outdiffusion. At higher coverages, the diffusing interface species are identified independently of possible subsurface Al motion.

broadening characteristic of multiple chemical shifts. Thus Volmer-Weber (simple islands) or Stranski-Krastanov (islands on plane monolayers) modes<sup>68</sup> of Au film growth appear unlikely.

The deposition of Au also changes the relative Ga 3d, As 3d, and Al 2p integrated peak intensities  $I_{\text{Ga}}^{3d}(h\nu)$ ,  $I_{\text{As}}^{3d}(h\nu)$ , and  $I_{\text{Al}}^{2p}(h\nu)$ , respectively. Figure 4 illustrates the ratios  $I_{\text{Ga}}^{3d}(130)/I_{\text{Al}}^{2p}(130)$ ,  $I_{\text{As}}^{3d}(130)/I_{\text{Al}}^{2p}(130)$ , and  $I_{\text{Ga}}^{3d}(130)/I_{\text{As}}^{3d}(130)$  as a function of metal overlayer coverage. Each peak height is normalized with respect to incident photon flux with the background subtracted. Both  $I_{\text{Ga}}^{3d}(130)/I_{\text{Al}}^{2p}(130)$  and  $I_{\text{As}}^{3d}(130)/I_{\text{Al}}^{2p}(130)$  decrease markedly (e.g., by 22% and 28%, respectively) with initial Au deposition. Assuming an immobile Al marker, these decreases are consistent only with a diffusion of Au atoms past the reacted Al interface layer into the GaAs. The inset in Fig. 4 illustrates this process.

These ratios exhibit some increase with additional Au coverage. For 1 Å Al on GaAs(110),  $I_{\text{Ga}}^{3d}(130)/I_{\text{Al}}^{2p}(130)$  increases with respect to  $I_{\text{As}}^{3d}(130)/I_{\text{Al}}^{2p}(130)$  with increasing Au coverage. This Ga/As nonstoichiometry is illustrated by the lower curve of  $I_{\text{Ga}}^{3d}(130)/I_{\text{As}}^{3d}(130)$  in Fig. 4. The Ga/As nonstoichiometry for 8 Å Au on 1 Å Al on GaAs(110) is 24% relative to the Al/GaAs surface with no Au. A larger Ga 3d versus As 3d escape depth accounts for only 11% of this increase with 8 Å and at  $h\nu = 130$  eV.<sup>35</sup> With  $h\nu = 80$  eV, the escape depth asymmetry is reversed, yet (as shown in Fig. 5) the Ga/As nonstoichiometry is still at least 9%. These results indicate that both Ga and As diffuse out of GaAs into the 8 Å Au overlayer,

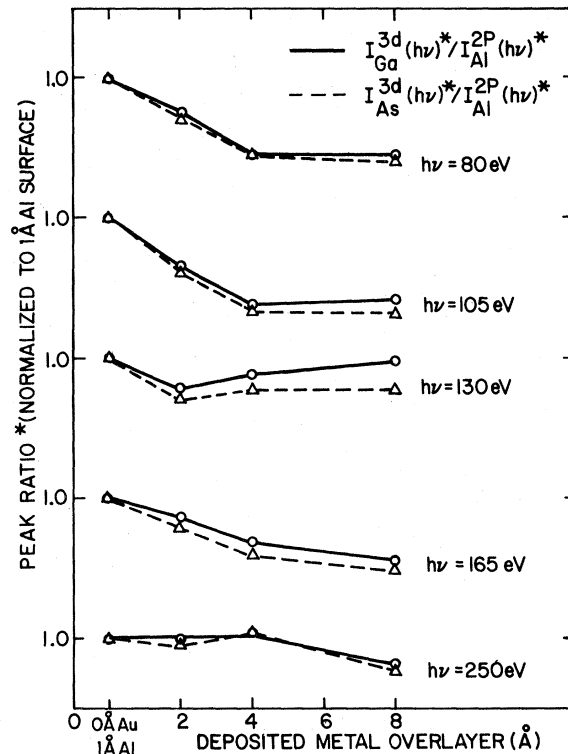


FIG. 5. Integrated peak-intensity ratios  $I_{\text{Ga}}^{3d}(h\nu)^*/I_{\text{Al}}^{2p}(h\nu)^*$  and  $I_{\text{As}}^{3d}(h\nu)^*/I_{\text{Al}}^{2p}(h\nu)^*$  normalized to the 1 Å Al surface and as a function of metal overlayer coverage for  $h\nu = 80, 105, 130, 165,$  and  $250$  eV.

consistent with the free Ga and As core-level features shown in Fig. 1, and that Ga diffuses faster than As relative to a 1 Å Al marker layer.

The increase in the Fig. 4 ratios coupled with the core-electron chemical shifts discussed above indicate that Ga and As must be present in the Au overlayer even if Al were liberated upon Au deposition. Thus at coverages above 2 Å, the diffusion of Au into the substrate GaAs and outdiffusion of the substrate constituents into the overlayer is also deduced without assuming that the Al is an immobile marker.

The initial diffusion of Au past the predeposited Al into GaAs is evident for a wide range of incident photon energies  $h\nu$ . For  $h\nu = 80, 105, 130, 165,$  and  $250$  eV, both  $I_{\text{Ga}}^{3d}(h\nu)^*/I_{\text{Al}}^{2p}(h\nu)^*$  and  $I_{\text{As}}^{3d}(h\nu)^*/I_{\text{Al}}^{2p}(h\nu)^*$  (the asterisk denotes normalization) to the 1 Å Al surface decrease with initial Au deposition. These effects are most pronounced for  $h\nu$  around 130 eV, where the scattering length of photoemitted Ga 3d and As 3d electrons is near a minimum<sup>36</sup> and therefore where surface sensitivity is highest. Conversely, such effects are minimized for  $h\nu = 250$  eV, where the escape depth is significantly larger. Therefore the decrease of these ratios with Au coverage for all  $h\nu$  in Fig. 5 cannot be due

to variations of photoelectron cross sections, but instead must be due to initial diffusion of Au into the GaAs lattice.

The nonstoichiometric Ga versus As outdiffusion in Figs. 4 and 5 is not characteristic of Au on GaAs(110) with no Al interlayer. For coverages above  $0.7 \text{ \AA}$  ( $\frac{1}{2}$  GaAs monolayer), the Ga/As ratio is enhanced by the presence of the Al interlayer.<sup>34</sup> Below this coverage, the Ga-to-As nonstoichiometry is in fact reversed. This is interpreted in terms of both "chemical trapping" of As and dipole-induced electromigration.<sup>64</sup> Nevertheless, Au diffuses into GaAs—as evidenced by the initial decrease of  $I_{\text{Ga}}^{3d}(h\nu)/I_{\text{Al}}^{2p}(h\nu)$  and  $I_{\text{As}}^{3d}(h\nu)/I_{\text{Al}}^{2p}(h\nu)$ —for initial Au deposition on all Al interlayer thicknesses measured.<sup>64</sup>

We have also used the variable excitation energy of the synchrotron source to probe the distribution of Ga and As within the Au overlayer. Figure 6 and 7 illustrate variations of the Ga 3d and As 3d integrated peak intensities, respectively, as a function of incident photon energy. These figures illustrate the gradual changes in  $I_{\text{Ga}}^{3d}(h\nu)$  and

$I_{\text{As}}^{3d}(h\nu)$  with increasing metal coverage. Similarly, only gradual changes occur for  $I_{\text{Al}}^{2p}(h\nu)$  with increasing Au coverage as shown in Fig. 8. Note that monochromator transmission, escape depth, and resolution factors are not factored into these curves. The curves for cleaved GaAs(110) and  $1 \text{ \AA}$  Al in each figure show the reproducibility of the integrated peak-intensity measurements for two separate cleavages. Between coverages of  $1 \text{ \AA}$  Al and  $8 \text{ \AA}$  Au +  $1 \text{ \AA}$  Al, both  $I_{\text{Ga}}^{3d}(h\nu)$  and  $I_{\text{As}}^{3d}(h\nu)$  exhibit relative increases in the range of 60–100 eV kinetic energy. These increased peak intensities in the energy range of highest surface sensitivity are due to a preferential segregation of Ga and As toward the free surface.

In contrast,  $I_{\text{Al}}^{2p}(h\nu)$  exhibits no substantial changes with increasing metal coverage as seen in Fig. 8. [The difference between  $I_{\text{Al}}^{2p}(130) \big|_{2 \text{ \AA Au}}$  and  $I_{\text{Al}}^{2p}(130) \big|_{4 \text{ \AA Au}}$  is the only exception to the otherwise regular curves. It does not correlate with the variations in Fig. 4.] These curves confirm that Al atoms do not move relative to the surface with Au deposition. The  $1 \text{ \AA}$  Al curve exhibits virtually

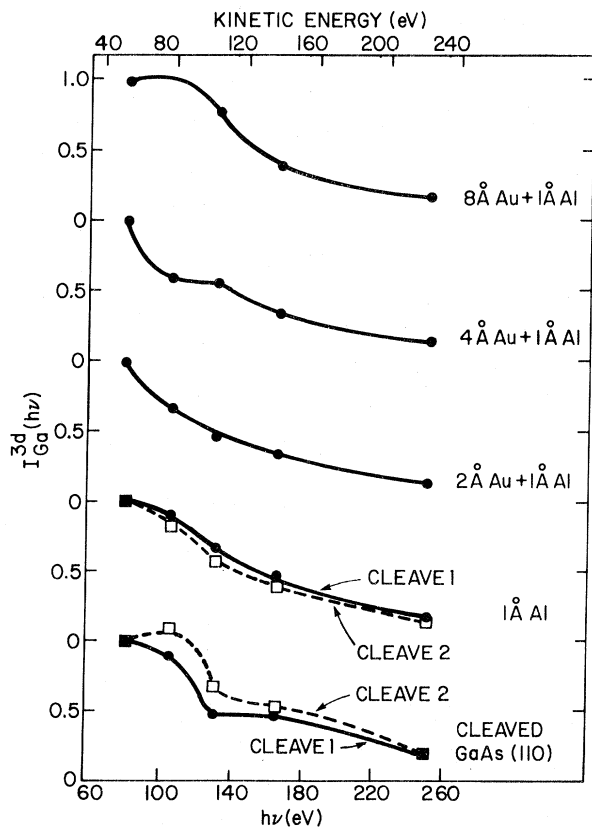


FIG. 6. Integrated peak intensities  $I_{\text{Ga}}^{3d}(h\nu)$  as a function of incident photon energy  $h\nu$  for various Al and Au coverages on cleaved GaAs(110). Each curve is normalized to  $I_{\text{Ga}}^{3d}(80)$ .

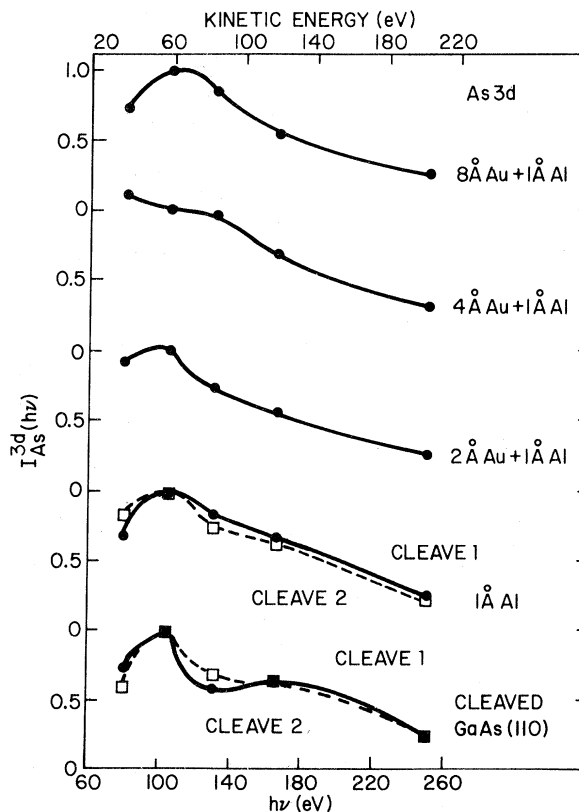


FIG. 7. Integrated peak intensities  $I_{\text{As}}^{3d}(h\nu)$  as a function of incident photon energy  $h\nu$  for various Al and Au coverages on cleaved GaAs(110). Each curve is normalized to  $I_{\text{As}}^{3d}(80)$ .

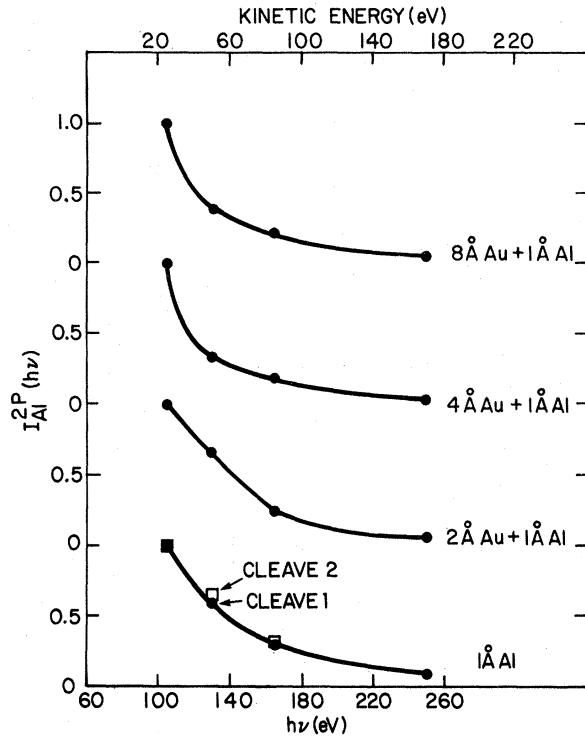


FIG. 8. Integrated peak intensities  $I_{Al}^{2p}(h\nu)$  as a function of incident photon energy  $h\nu$  for various Al and Au coverages on cleaved GaAs(110). Each curve is normalized to  $I_{Al}^{2p}(80)$ .

identical  $I_{Al}^{2p}(h\nu)$  variations for two separate cleavages, again demonstrating the reproducibility of these measurements.

The  $I_{Ga}^{3d}(h\nu)$  and  $I_{As}^{3d}(h\nu)$  data in Figs. 6 and 7 provide information on the distribution of Ga relative to As within the surface layers. A measure of this relative distribution is the  $I_{Ga}^{3d}(h\nu)/I_{As}^{3d}(h\nu)$  ratio for each surface, which cancels out any (small) differences in the geometry of data collection from surface to surface. Furthermore, to compensate for the different energy dependences of the Ga 3d and As 3d photoelectron cross sections, we have normalized a given surface's  $I_{Ga}^{3d}(h\nu)$  and  $I_{As}^{3d}(h\nu)$  with respect to a reference surface. Here we choose the 1 Å Al/GaAs surface rather than the cleaved GaAs surface to account for any final-state effects of the Al layer on the Ga 3d and As 3d cross sections. Figure 9 illustrates the normalized  $R(h\nu) = [I_{Ga}^{3d}(h\nu)/I_{Ga}^{3d}(h\nu)|_{1\text{Å Al}}] / [I_{As}^{3d}(h\nu)/I_{As}^{3d}(h\nu)|_{1\text{Å Al}}]$  for the various metal overlayers on cleaved GaAs(110). By definition,  $R(h\nu)$  is a straight line for the 1 Å Al surface.

$R(h\nu)$  should also be relatively insensitive to changes in Ga and As environment with increasing metal coverage which could alter the escape probability for Ga versus As photoelectrons. Between

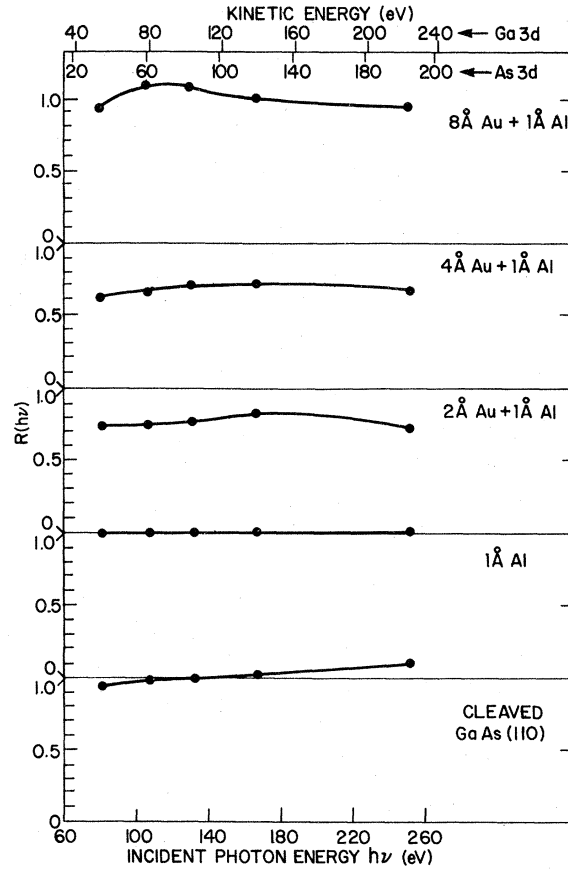


FIG. 9. Normalized ratio of integrated peak intensities  $R(h\nu) = [I_{Ga}^{3d}(h\nu)/I_{Ga}^{3d}(h\nu)|_{1\text{Å Al}}] / [I_{As}^{3d}(h\nu)/I_{As}^{3d}(h\nu)|_{1\text{Å Al}}]$  as a function of incident photon energy  $h\nu$  for various Al and Au coverages on cleaved GaAs(110). Top scale gives the kinetic energy of photoemitted Ga 3d and As 3d electrons for a given photon energy.

kinetic energies of 50 and 500 eV, changes in electron scattering length with material are quite small.<sup>36</sup> Likewise the partial photoionization cross sections of the Ga and As 3d core levels are quite similar and vary smoothly in this energy region.<sup>69</sup> As a result, changes in chemical environment are expected to affect  $I_{Ga}^{3d}(h\nu)$  and  $I_{As}^{3d}(h\nu)$  in the same way. Furthermore, any (small) differences between Ga and As are minimized by taking their ratio.

All variations in  $R(h\nu)$  in Fig. 9 are therefore due to the different spatial distribution of Ga and As below the surface. Their relative contribution to the Ga 3d and As 3d photoemission changes as the escape depth varies with photoelectron kinetic energy. If Ga and As were distributed uniformly within the Au overlayer, one would expect these curves to be horizontal lines. The scale above Fig. 9 provides the kinetic energies of Ga 3d and As 3d electrons for a given  $h\nu$ . Since the minimum



in the electron escape depth for GaAs (Refs. 35 and 70) lies at 50–80 eV, core-level intensities represent increasing contributions from the bulk with increasing kinetic energy above this range and decreasing energy below it

Relative to the 1 Å Al curve, the  $R(h\nu)$  curves exhibit only gradual changes at 2 Å Au and 4 Å Au overlayers. For 8 Å Au coverage, however,  $R(h\nu)$  exhibits a well-defined maximum at  $h\nu = 105\text{--}130$  eV corresponding to the most surface-sensitive kinetic energies. This establishes that more Ga than As resides on or near the Au-vacuum interface independent of the presence of the Al interlayer. Furthermore, this spatial nonstoichiometry occurs only after 4–8 Å thicknesses of Au are deposited.

The 1 Å Al and cleaved surfaces exhibit no strong differences, although the  $R(80)$  increase with 1 Å Al deposition may correspond to slightly more Ga than As on the Al/GaAs surface since the Ga 3*d* photoelectrons have a slightly shorter escape depth than As 3*d* photoelectrons at  $h\nu = 80$  eV. Likewise, the  $R(250)$  decrease with 1 Å Al deposition may result from the slightly longer escape depth of Ga 3*d* vs As 3*d* photoelectrons at  $h\nu = 250$  eV. This is consistent with the measured exchange reaction.<sup>10, 52, 53</sup>

The variation in  $R(h\nu)$  with increasing Au coverage in Fig. 9 suggests that the spatial distribution of Ga and As is a function of the Au overlayer thickness. Thus, depth profiling experiments which measure elemental composition as surface layers are sputtered away,<sup>41</sup> will very likely perturb the thermodynamic equilibrium of an elemental distribution on this atomic scale. This fact serves to enhance the utility of the SXPS-marker technique for nondestructive depth profiling.

#### IV. DISCUSSION

The SXPS spectra demonstrate that microscopic diffusion measurements can effectively be made even at room temperature. The variations of core-level intensity with  $h\nu$  and overlayer thickness reveal that both Au indiffusion and Ga and As outdiffusion take place at Au/GaAs interfaces. The SXPS evidence for free Ga and As coupled with the nonstoichiometric outdiffusion demonstrates that Ga and As diffuse through the Au overlayer as atoms and not as molecular species. Likewise, the diffusion of Au past the Al with multilayer Au overlayers shows that the “atomic-like” Au spectral features correspond to Au dispersal in the GaAs lattice. There is no way for these Au atoms to diffuse past the Al interlayer and remain dispersed “on” but not “in” the GaAs surface.

The use of interlayer atoms to characterize

atomic interdiffusion through the establishment of an immobile marker layer is valid only when there is supporting evidence that the marker itself does not move. In the case of Al submonolayers at Au/GaAs (110) interface, the SXPS data is consistent with a stationary Al layer. First, the Al 2*p* core level does not shift to lower binding energy with Au deposition, as would be expected if Al were to dissociate and drift into the Au overlayer. Indeed, for Al coverages above 1 Å, such a chemically shifted peak does appear in the Al 2*p* spectrum with Au deposition.<sup>64</sup> This second peak corresponds to diffusion into the Au of the Al in excess of the Al bonded to the GaAs substrate. Thus the SXPS technique provides a positive check for dissociated Al bonded metallicity within the Au overlayer. If, on the other hand, the Al moved into the GaAs substrate substitutionally, the Al 2*p* core level should shift substantially to higher binding energy due to the higher bonding coordination.<sup>71</sup> The 0.4-eV shift in Fig. 1 (Al 2*p* peak relative to Ga and As 3*d* peaks) can easily be accounted for by the presence of the Au overlayer alone. Furthermore, diffusion of Al into the GaAs substrate would produce an *increase* in  $I_{\text{Ga}}^{3d}(130)/I_{\text{Al}}^{2p}(130)$  and  $I_{\text{As}}^{3d}(130)/I_{\text{Al}}^{2p}(130)$ —exactly opposite to the changes observed. On this basis, we can rule out simple substitutional indiffusion of Al as well.

A second possible method of Al motion involves diffusion of *both* Al and As into the Au overlayer and covalent bonding between them. In this case the AlAs bonding and thereby the characteristic Al 2*p* core-level shift might be preserved. However, AlAs diffusion into the Au as molecules is quite unlikely. Likewise, several factors argue against dissociation of both Al and As at the interface, diffusion into the Au as atoms, and recombination near the Au film’s surface. Both processes require at least as much As as Al near the Au surface since all the Al is strongly bonded. Yet as Fig. 4 shows,  $I_{\text{As}}^{3d}(130)/I_{\text{Al}}^{2p}(130)$  actually decreases. Moreover, the As 3*d* core-level spectra in Fig. 1 indicates that much of this As is not strongly bonded.

Another possibility involves a dissociation of only a fraction of the chemisorbed Al and a re-bonding to but a fraction of the diffused As. In this case, we can estimate an upper limit for any dissociated Al. The 28% decrease of  $I_{\text{As}}^{3d}(130)/I_{\text{Al}}^{2p}(130)$  in Fig. 4, of which only  $< \frac{2}{3} I_{\text{As}}^{3d}(130)$  represents strongly bonded As, indicates that less than half of this decrease can be accounted for by possible Al dissociation. Similar measurements for a variety of submonolayer Al coverages with 20–Å thick Au overlayers on GaAs(110) establish that  $< 20\%$  of the  $I_{\text{As}}^{3d}(130)/I_{\text{Al}}^{2p}(130)$  decrease might be due to Al dissociation.<sup>72</sup> In some cases, this frac-

tion corresponds to, at most, a few percent of a monolayer.

Last of all, these interdiffusion results are confirmed by using Ti marker layers.<sup>72</sup> The same qualitative features of Fig. 4 are observed with Ti substituted for Al. Here again interdiffusion can be monitored because the marker atoms bond strongly with only one of the two interface media.

On the other hand, a eutectic may form with Ga, As, and Al in the now Au overlayer. In such an instance, outdiffusion of the substrate atoms would be expected. In this case, the Au would have substantially diffused as atoms into the GaAs substrate past the initially deposited Al layer. Therefore, the details available in these SXPS experiments provide a microscopic description of the diffusing interface species even if the interlayer does not remain immobile.

Several models have been proposed for the Au/GaAs interdiffusion and its relation to Schottky-barrier formation. The results of this study are in agreement with several experimental studies. At elevated temperatures for example, Magee and Peng observed intermixing of Au and GaAs and the formation of AuGa compounds with transmission electron microscopy (TEM) after a 550 °C anneal.<sup>23</sup> Likewise, Sinha and Poate found both Au indiffusion and Ga outdiffusion for interfaces annealed at 250 °C or higher.<sup>19</sup> Robinson drew similar conclusions based on sputter profiling with AES on interfaces annealed at 372 °C.<sup>26</sup> Hiraki *et al.* observed Ga and As on Au/GaAs surfaces at room temperature but could not characterize any diffusion into GaAs.<sup>28</sup> Sputter profiles using AES reveal an excess of Ga near the surface of thick Au films on GaAs at room temperature.<sup>30,31</sup> The SXPS-marker results suggest that Waldrop and Grant's XPS measurements showing only As present on Au/GaAs films<sup>59</sup> are not representative of the initial diffusion process. Nevertheless, for Al marker layers of  $\frac{1}{2}$ -monolayer coverage or less, As diffusion exceeds Ga diffusion into the Au overlayer.<sup>34</sup> The Ga excess observed by various methods at surfaces of thick Au films on GaAs may be due to As sublimation (especially for the annealed interfaces),<sup>73</sup> interface contamination,<sup>34</sup> and nonstoichiometry introduced during sputter cleaning<sup>74</sup> of the GaAs surface.<sup>75</sup>

The interdiffusion effects reported here determine the electronic changes observed at the microscopic Au/GaAs interface. In particular, these include the metal-induced surface states,<sup>13</sup> the movement of the Fermi level with respect to the band edges,<sup>5,30</sup> and the interface dipole formation<sup>11</sup> with the first few monolayers of metal deposited. In turn, these effects at microscopic coverages determine the Schottky-barrier height of the mac-

roscopic junction.

The movement of Au into GaAs during the initial stage of interdiffusion is strong evidence that Au within the GaAs lattice is electrically active and plays a central role in forming the Schottky barrier of this relatively unreactive<sup>11,33</sup> interface. The initial Au diffusion into GaAs is consistent with its relatively high diffusion coefficient extrapolated to room temperature.<sup>76</sup> The subsequent Ga and As outdiffusion at higher Au coverages suggests that these electronic charges take place via Au association with Ga and/or As vacancies. In fact, Sokolov and Shilshiyau attribute the high diffusion coefficient during the initial stages of Au/GaAs diffusion to interstitial Au filling surface vacancies in semiconductor layers near the surface.<sup>17</sup> The rates of diffusion for Au, Ga, and As in GaAs are several orders of magnitude larger than the diffusion coefficients calculated at room temperature.<sup>77</sup> Moreover, the interdiffusion occurs well below the eutectic temperatures of any possible alloys.<sup>78,79</sup> Nevertheless, Au does dissociate both Ga and As at the GaAs interface and promotes free Ga and As movement through the metal. Such phenomena suggest a different mode of diffusion for these species at room versus elevated temperatures.

The SXPS-marker measurements are in accord with Rutherford backscattering<sup>15,19</sup> and AES sputter-profile<sup>20</sup> observations of both Au and Ga interdiffusion. Capacitance-voltage ( $C-V$ ) and current-voltage ( $I-V$ ) measurements of the Au-GaAs barrier height also confirm the presence of charged traps and an  $n^+$  layer near the GaAs surface.<sup>80,81</sup> These interdiffusion results are contrary to the conclusions of Madams *et al.*<sup>82</sup> and Guha *et al.*<sup>27</sup> who attribute the Schottky-barrier height and its decrease with annealing to Ga diffusion and vacancy formation alone. Simple Ga (As) vacancies cannot account for the donor (acceptor) level pinning attributed to metals on  $n$ -type GaAs (Ref. 83) since As vacancies are donors and Ga vacancies are acceptors in GaAs.<sup>84</sup> Instead, complexes such as antisite defects<sup>30,85</sup> or Au impurities at GaAs defect sites must account for the electrical behavior. Evidence for the latter derives from measurements of the electrical activity of Au in GaAs. Hiesinger<sup>86</sup> detected a deep acceptor level at 0.4 eV above the valence-band edge  $E_v$  (1 eV below the conduction-band edge  $E_c$ ) as well as a shallow acceptor level 0.05 eV above  $E_v$  via Hall-effect measurements of Au-doped GaAs. The deep level lies close to the position of the Fermi level at the macroscopic Au-GaAs junction (0.9 eV below  $E_c$ ).<sup>87</sup> Borrego *et al.* inferred from  $C-V$  measurements that Au on GaAs produced deep donors 0.9–1.2 eV below  $E_c$  within the GaAs band gap.<sup>88</sup> The forma-

tion of such electrically active impurity levels due to Au atoms in GaAs is not inconsistent with the narrow range of Schottky-barrier heights reported for metals on GaAs.<sup>87</sup> Hjalmarson *et al.* have recently shown that the energies of deep levels are determined primarily by the host atoms surrounding the impurity and not the impurity itself.<sup>89</sup>

In conclusion, we have monitored the atomic motion of Au, Ga, and As during the initial stages of interdiffusion at the microscopic Au/GaAs(110) interface in the presence of a submonolayer concentration of Al at the interface, which does not substantially affect<sup>34</sup> the diffusion process. We have established that Au diffusing into the GaAs lattice with initial deposition must be associated with the observed electronic charges induced by the metal as well as with the Schottky-barrier

formation. We have also described the spatial redistribution of Ga and As atoms near the microscopic Au/GaAs interface in a nondestructive way and at room temperature. These results demonstrate that SXPS-marker measurements are a powerful new technique for probing metal-semiconductor interfaces.

#### ACKNOWLEDGMENTS

This work was supported in part by National Science Foundation Grant No. DMR 73-07692 in collaboration with the Stanford Linear Accelerator Center and the Energy Research Development Agency. We wish to thank the staff of the Stanford Synchrotron Radiation Laboratory for facilities support.

- <sup>1</sup>G. Margaritondo, J. E. Rowe, and S. B. Christman, *Phys. Rev. B* **14**, 5396 (1976).
- <sup>2</sup>J. E. Rowe, *J. Vac. Sci. Technol.* **13**, 798 (1976).
- <sup>3</sup>W. E. Spicer, P. E. Gregory, P. W. Chye, I. A. Babalola, and T. Sukegawa, *Appl. Phys. Lett.* **27**, 617 (1975).
- <sup>4</sup>P. W. Chye, I. A. Babalola, T. Sukegawa, and W. E. Spicer, *Phys. Rev. Lett.* **35**, 1602 (1975).
- <sup>5</sup>W. Gudat and D. E. Eastman, *J. Vac. Sci. Technol.* **13**, 831 (1976).
- <sup>6</sup>J. E. Rowe and G. Margaritondo, *Proceedings of the Seventh International Vacuum Congress and the Third International Conference on Solid Surfaces* (IVC, Vienna, 1977), p. 1191.
- <sup>7</sup>P. W. Chye, T. Sukegawa, I. A. Babalola, H. Sunami, P. Gregory, and W. E. Spicer, *Phys. Rev. B* **15**, 2118 (1977).
- <sup>8</sup>I. Lindau, P. W. Chye, C. M. Garner, P. Pianetta, and W. E. Spicer, *J. Vac. Sci. Technol.* **15**, 1332 (1978).
- <sup>9</sup>R. H. Williams, R. R. Varma, and V. Montgomery, *J. Vac. Sci. Technol.* **16**, 1418 (1979).
- <sup>10</sup>L. J. Brillson, R. Z. Bachrach, R. S. Bauer, and J. McMenamin, *Phys. Rev. Lett.* **42**, 397 (1979).
- <sup>11</sup>L. J. Brillson, *J. Vac. Sci. Technol.* **16**, 1137 (1979).
- <sup>12</sup>L. J. Brillson, *Phys. Rev. B* **18**, 2431 (1978).
- <sup>13</sup>L. J. Brillson, in *Proceedings of the Fourteenth International Conference on the Physics of Semiconductors*, edited by R. A. Stradling (Plessy, Edinburgh, 1978), p. 765.
- <sup>14</sup>L. J. Brillson, *J. Vac. Sci. Technol.* **15**, 1378 (1978).
- <sup>15</sup>A. K. Sinha and J. M. Poate, in *Thin Films—Interdiffusion and Reactions*, edited by J. M. Poate, K. N. Tu, and J. W. Mayer (Wiley-Interscience, New York, 1978), pp. 407 and references therein.
- <sup>16</sup>J. O. McCauldin, *J. Vac. Sci. Technol.* **11**, 990 (1974).
- <sup>17</sup>V. I. Boltaks and F. S. Shilshiyanu, *Fiz. Tverd. Tela* **5**, 2310 (1963) [*Sov. Phys.—Solid State* **5**, 1680 (1963)]; and V. I. Boltaks and F. S. Shilshiyanu, *Fiz. Tverd. Tela* **6**, 328 (1964) [*Sov. Phys.—Solid State* **6**, 265 (1964)].
- <sup>18</sup>J. Gyulai, J. W. Mayer, V. Rodriguez, A. Y. C. Yu, and H. J. Gopen, *J. Appl. Phys.* **42**, 3578 (1971).
- <sup>19</sup>A. K. Sinha and J. M. Poate, *Appl. Phys. Lett.* **23**, 666 (1973).
- <sup>20</sup>C. J. Todd, G. W. B. Ashwell, J. D. Speight and R. Heckingbottom, *Gallium Arsenide and Related Compounds, 1974* (Institute of Physics, London, 1974), Vol. 22, p. 171.
- <sup>21</sup>A. K. Sinha and J. M. Poate, *Proceedings of the Sixth International Vacuum Congress* [*Jpn. J. Appl. Phys. Suppl.* **2**, Pt. 1, 841 (1974)].
- <sup>22</sup>A. K. Sinha, T. E. Smith, and H. J. Levinstein, *IEEE Trans. Electron Devices* **ED-22**, 218 (1975).
- <sup>23</sup>T. J. Magee and J. Peng, *Phys. Status Solidi A* **32**, 695 (1975).
- <sup>24</sup>G. Y. Robinson, *Solid-State Electron.* **18**, 331 (1975).
- <sup>25</sup>H. B. Kim, G. C. Sweeney, and T. M. S. Heng, *Gallium Arsenide and Related Compounds, 1975* (Institute of Physics, London, 1975), Vol. 24, p. 307.
- <sup>26</sup>G. Y. Robinson, *J. Vac. Sci. Technol.* **13**, 884 (1976).
- <sup>27</sup>S. Guha, B. M. Arora, and V. P. Salvi, *Solid-State Electron.* **20**, 431 (1977).
- <sup>28</sup>A. Hiraki, K. Shuto, S. Kim, W. Kammura, and W. Iwami, *Appl. Phys. Lett.* **31**, 611 (1977).
- <sup>29</sup>P. W. Chye, I. Lindau, P. Pianetta, C. M. Garner, and W. E. Spicer, *Phys. Rev. B* **17**, 2682 (1978).
- <sup>30</sup>P. W. Chye, I. Lindau, P. Pianetta, C. M. Garner, C. Y. Su, and W. E. Spicer, *Phys. Rev. B* **18**, 5545 (1978).
- <sup>31</sup>A. Hiraki, S. Kim, W. Kammura, and M. Iwami, *Surf. Sci.* **86**, 706 (1979).
- <sup>32</sup>L. J. Brillson, *Phys. Rev. Lett.* **38**, 245 (1977).
- <sup>33</sup>L. J. Brillson, *Phys. Rev. Lett.* **40**, 260 (1978).
- <sup>34</sup>L. J. Brillson, G. Margaritondo, and N. G. Stoffel, *Phys. Rev. Lett.* **44**, 667 (1980).
- <sup>35</sup>L. J. Brillson, R. S. Bauer, R. Z. Bachrach, and G. Hansson, *Appl. Phys. Lett.* **36**, 326 (1980).
- <sup>36</sup>I. Lindau and W. E. Spicer, *J. Electron Spectrosc.* **3**, 409 (1974).
- <sup>37</sup>See, for example, R. S. Bauer, J. C. McMenamin, H. Peterson, and A. Bianconi, in *Proceedings of the International Topical Conference on SiO<sub>2</sub> and Its Interfaces*, edited by S. Pantelides (Pergamon, New York, 1978), p. 401.

- <sup>38</sup>W. K. Chu, J. W. Mayer, and M. A. Nicolet, *Backscattering Spectrometry* (Academic, New York, 1977).
- <sup>39</sup>S. A. Schwartz, C. R. Helms, W. E. Spicer, and N. J. Taylor, *J. Vac. Sci. Technol.* **15**, 227 (1978).
- <sup>40</sup>H. Liebl, *J. Vac. Sci. Technol.* **12**, 385 (1975).
- <sup>41</sup>G. K. Wehner, in *Methods of Surface Analysis*, edited by A. W. Czanderna (Elsevier, Amsterdam, 1975).
- <sup>42</sup>J. M. Poate and T. C. Tisone, *Appl. Phys. Lett.* **24**, 391 (1974).
- <sup>43</sup>F. D'Heurle and R. Rosenberg, in *Physics of Thin Films*, edited by G. Haas, M. Francombe, and R. Hoffman (Academic, New York, 1973), Vol. 7, p. 257.
- <sup>44</sup>G. J. van Gurp, D. Sigurd, and W. F. van der Weg, *Appl. Phys. Lett.* **29**, 159 (1973).
- <sup>45</sup>C. J. Kirchner, J. W. Mayer, K. N. Tu, and J. F. Ziegler, *Appl. Phys. Lett.* **22**, 81 (1973).
- <sup>46</sup>W. K. Chu, S. S. Lau, J. W. Mayer, H. Muller, and K. N. Tu, *Thin Solid Films* **25**, 393 (1975).
- <sup>47</sup>K. N. Tu, *Appl. Phys. Lett.* **27**, 221 (1975).
- <sup>48</sup>S. S. Lau, J. S. Feng, J. O. Olowolafe, and M. A. Nicolet, *Thin Solid Films* **25**, 415 (1975).
- <sup>49</sup>R. Pretorius, C. L. Ramiller, S. S. Lau, and M. A. Nicolet, *Appl. Phys. Lett.* **30**, 501 (1977).
- <sup>50</sup>R. Pretorius, Z. L. Liao, S. S. Lau, and M. A. Nicolet, *J. Appl. Phys.* **48**, 2886 (1977).
- <sup>51</sup>J. Baglin, F. d'Heurle, and S. Petersson, *Appl. Phys. Lett.* **33**, 289 (1978).
- <sup>52</sup>R. Z. Bachrach, *J. Vac. Sci. Technol.* **15**, 1340 (1978).
- <sup>53</sup>R. Z. Bachrach, R. S. Bauer, J. C. McMenamin, and A. Bianconi, in *Proceedings of the Fourteenth International Conference on the Physics of Semiconductors*, edited by R. A. Stradling (Plessey, Edinburgh, 1978), p. 1073.
- <sup>54</sup>E. J. Mele and J. D. Joannopoulos, *Phys. Rev. Lett.* **42**, 1094 (1979).
- <sup>55</sup>E. J. Mele and J. D. Joannopoulos, *J. Vac. Sci. Technol.* **16**, 1154 (1979).
- <sup>56</sup>D. D. Wagman, W. H. Evans, V. B. Parker, I. Halow, S. M. Bailey, and R. H. Schumm, *Selected Values of Chemical Thermodynamic Properties*, National Bureau of Standards, Technical Notes 270-3-270-7 (U.S. G.P.O., Washington, D.C., 1968-71).
- <sup>57</sup>A. Yazawa and Y. K. Lee, *Trans. Japan Inst. Met.* **11**, 411 (1970).
- <sup>58</sup>S. U. Campisano, G. Foti, E. Rimini, S. S. Lau, and J. W. Mayer, *Philos. Mag.* **31**, 903 (1975).
- <sup>59</sup>J. R. Waldrop and R. W. Grant, *Appl. Phys. Lett.* **34**, 630 (1979).
- <sup>60</sup>F. C. Brown, R. Z. Bachrach, S. B. M. Hagstrom, N. Lien, and C. H. Pruett, in *Vacuum Ultraviolet Radiation Physics*, edited by E. Koch, R. Haensel, and C. Kunz (Pergamon, Elmsford, New York, 1975), p. 785.
- <sup>61</sup>P. Pianetta, I. Lindau, C. M. Garner, and W. E. Spicer, *Phys. Rev. Lett.* **37**, 1166 (1976).
- <sup>62</sup>G. Margaritondo, L. J. Brillson, and N. G. Stoffel, *Proceedings of the Sixth International Conference on Vacuum Ultraviolet Radiation Physics* (University of Virginia, Charlottesville, Va., 1980) I-16; G. Margaritondo, L. J. Brillson, N. G. Stoffel, and A. D. Katnani, *Solid State Commun.* **35**, 277 (1980).
- <sup>63</sup>L. J. Brillson, R. S. Bauer, R. Z. Bachrach, and J. C. McMenamin, *J. Vac. Sci. Technol.* **17**, 476 (1980).
- <sup>64</sup>L. J. Brillson, G. Margaritondo, N. G. Stoffel, R. S. Bauer, R. Z. Bachrach, and G. Hansson, *J. Vac. Sci. Technol.* **17**, 880 (1980).
- <sup>65</sup>P. R. Skeath, C. Y. Su, P. W. Chye, I. Lindau, and W. E. Spicer, *J. Vac. Sci. Technol.* **16**, 1143 (1979).
- <sup>66</sup>K. S. Liang, W. R. Salaneck, and I. A. Aksay, *Solid State Commun.* **19**, 329 (1976) and references therein.
- <sup>67</sup>Band bending and interfacial dipole voltages can be separated via photoinduced band flattening; see, for example, L. J. Brillson and D. L. Kruger, *Surf. Sci.* **102**, 518 (1981).
- <sup>68</sup>See, for example, C. A. Neugebauer, in *Handbook of Thin Film Technology*, edited by L. I. Maissel and R. Glang (McGraw-Hill, New York, 1970), pp. 8-1.
- <sup>69</sup>I. Lindau, P. Pianetta, and W. E. Spicer, *Proceedings of the International Conference on Physics of X-ray Spectra*, edited by R. D. DesLattes (U.S.G.P.O., Washington, D.C., 1976), p. 78.
- <sup>70</sup>P. Pianetta, Ph.D. thesis, Stanford University, 1976, unpublished.
- <sup>71</sup>A. Kahn, L. J. Brillson, G. Margaritondo, and A. D. Katnani, *Solid State Commun.* (in press).
- <sup>72</sup>L. J. Brillson, G. Margaritondo, C. F. Brucker, N. G. Stoffel, and A. D. Katnani, unpublished.
- <sup>73</sup>E. Kinsbron, P. K. Gallagher, and A. T. English, *Solid State Electron.* **22**, 517 (1979).
- <sup>74</sup>L. J. Brillson, *Surf. Sci.* **51**, 45 (1975).
- <sup>75</sup>J. L. Singer, J. S. Murday, and L. R. Cooper, *J. Vac. Sci. Technol.* **15**, 725 (1978).
- <sup>76</sup>P. D. Vyas and B. L. Sharma, *Thin Solid Films* **51**, L21 (1978).
- <sup>77</sup>D. L. Kendall, in *Semiconductors and Semimetals*, edited by R. K. Willardson and A. C. Beer (Academic, New York, 1968), Vol. 4, p. 163.
- <sup>78</sup>M. B. Panish, *J. Electrochem. Soc.* **114**, 516 (1967).
- <sup>79</sup>M. Hansen and K. Anderko, *Constitution of Binary Alloys*, 2nd ed. (McGraw-Hill, New Jersey, 1958).
- <sup>80</sup>C. R. Crowell and V. L. Rideout, *Solid-State Electron.* **12**, 89 (1969).
- <sup>81</sup>F. A. Padovani and R. Stratton, *Solid-State Electron.* **9**, 695 (1966).
- <sup>82</sup>C. J. Madams, D. V. Morgan, and M. J. Howes, *Electron. Lett.* **11**, 574 (1975).
- <sup>83</sup>W. E. Spicer, I. Lindau, P. Skeath, C. Y. Su, and P. Chye, *Phys. Rev. Lett.* **44**, 420 (1980).
- <sup>84</sup>S. Y. Chiang and G. L. Pearson, *J. Appl. Phys.* **46**, 2986 (1975).
- <sup>85</sup>J. A. van Vechten, *J. Electrochem. Soc.* **122**, 419 (1975).
- <sup>86</sup>P. Hiesinger, *Phys. Status Solidi A* **33**, K 39 (1976).
- <sup>87</sup>C. A. Mead, *Solid-State Electron.* **9**, 1023 (1966).
- <sup>88</sup>J. M. Borrego, R. J. Gutman, and S. Ashok, *Solid-State Electron.* **20**, 125 (1977).
- <sup>89</sup>H. P. Hjalmarsen, R. E. Allen, H. Büttner, and J. D. Dow, *J. Vac. Sci. Technol.* **17**, 993 (1980).